



HAL
open science

Competing phases in BiFeO₃ thin films under compressive epitaxial strain

B. Dupé, Infante I. Canero, G. Geneste, P.E. Janolin, M. Bibes, A. Barthelemy, S. Lisenkov, L. Bellaiche, S. Ravy, B. Dkhil

► **To cite this version:**

B. Dupé, Infante I. Canero, G. Geneste, P.E. Janolin, M. Bibes, et al.. Competing phases in BiFeO₃ thin films under compressive epitaxial strain. *Physical Review B: Condensed Matter and Materials Physics* (1998-2015), 2010, 81 (144128), pp.144128-5. 10.1103/pHYsrEVb.81.144128 . hal-00577838

HAL Id: hal-00577838

<https://hal.science/hal-00577838>

Submitted on 17 Mar 2011

HAL is a multi-disciplinary open access archive for the deposit and dissemination of scientific research documents, whether they are published or not. The documents may come from teaching and research institutions in France or abroad, or from public or private research centers.

L'archive ouverte pluridisciplinaire **HAL**, est destinée au dépôt et à la diffusion de documents scientifiques de niveau recherche, publiés ou non, émanant des établissements d'enseignement et de recherche français ou étrangers, des laboratoires publics ou privés.

Competing phases in BiFeO₃ thin films under compressive epitaxial strain

B. Dupé,¹ I. C. Infante,² G. Geneste,^{3,1} P.-E. Janolin,¹ M. Bibes,² A. Barthélémy,² S. Lisenkov,⁴ L. Bellaiche,⁵ S. Ravy,⁶ and B. Dkhil¹

¹Laboratoire Structures, Propriétés et Modélisation des Solides, UMR 8580, CNRS-École Centrale Paris, Grande Voie des Vignes, 92295 Châtenay-Malabry Cedex, France

²Unité Mixte de Physique CNRS/Thales, Campus de l'École Polytechnique, 1 Av. A. Fresnel, 91767 Palaiseau, France and Université Paris-Sud 11, 91405 Orsay, France

³CEA, DAM, DIF, F-91297 Arpaçon, France

⁴Department of Physics, University of South Florida, Tampa, Florida 33620, USA

⁵Physics Department, University of Arkansas, Fayetteville, Arkansas 72701, USA

⁶Synchrotron Soleil, L'Orme des Merisiers, Saint-Aubin BP 48, 91192 Gif-sur-Yvette Cedex, France

(Received 9 February 2010; revised manuscript received 7 April 2010; published 30 April 2010)

Combining density-functional calculations and x-ray diffraction experiments, we show that BiFeO₃ epitaxially grown under compressive strain on cubic substrates evolves from the monoclinic *Cc* phase (resulting from the strain-induced deformation of the ground-state rhombohedral *R3c* phase) to the monoclinic *Cm* phase with increasing misfit, the transition being at about -4.5% / -5.5% . Moreover, the polarization of the *Cc* phase only rotates (instead of increasing) for misfit strain ranging from 0% to -4% , due to a strong coupling between polar displacements and oxygen octahedra tilts. This strong interaction is of interest for multiferroics where usually both structural degrees of freedom coexist.

DOI: [10.1103/PhysRevB.81.144128](https://doi.org/10.1103/PhysRevB.81.144128)

PACS number(s): 77.80.-e, 68.55.Nq, 61.05.cp, 75.50.Ee

I. INTRODUCTION

Multiferroics are currently gaining more and more attention because they display simultaneously magnetic, polar, and structural order parameters, whose coupling is at the origin of their multifunctional properties.^{1,2} In particular, much effort is being made toward the control of these properties by means of electric and magnetic fields, allowing to explore several concepts and devices in the field of spintronic, microwave filters or electromechanical sensors and actuators.³⁻⁵ Furthermore, significant experimental and theoretical efforts are also directed to obtain a better understanding of the coupling mechanisms between the different degrees of freedom, and this challenging area is one of the most active in the field of material sciences.⁶⁻⁸ BiFeO₃ (BFO) is one of the most promising multiferroics for technology applications and fundamental interest⁹ since the polar and magnetic ordering coexist at room temperature. Below the Curie temperature $T_C \approx 1100$ K, the crystal structure of the polar phase of BFO bulk is described by the rhombohedral space group *R3c*, which allows antiphase octahedral tilting and ionic displacements from the centrosymmetric positions about and along a same $\langle 111 \rangle_C$ direction (cubic notation). At room temperature, the bulk polarization reaches $\approx 100 \mu\text{C}/\text{cm}^2$.¹⁰ Although the *R3c* symmetry allows the existence of a weak ferromagnetic moment, a cycloid-type spatial spin modulation, superimposed to the G-type antiferromagnetic spin ordering occurring below the Néel temperature T_N of about 640 K,¹¹ prevents the observation of any net magnetization. When BFO is deposited as a thin film, while a weak ferromagnetism appears as a result of the annihilation of the cycloid modulation through the epitaxial strains,¹² the polarization is barely affected whereas one would anticipate a huge enhancement. Indeed, previous works have already suggested the possibility of BFO systems having very large

polarization and axial ratio,¹³ in particular, an hypothetical tetragonal *P4mm* phase, which would exhibit very large ferroelectric distortions and a very large polarization $\approx 150 \mu\text{C}/\text{cm}^2$.^{14,15} Interestingly, starting from this phase and allowing in-plane polar displacements (along $[110]$), one obtains a monoclinic phase with *Cm* symmetry that could be more stable. Note that such latter monoclinic *Cm* state has been reported,¹⁶ despite some controversial issues. Actually, the precise conditions in which such BFO phases might exist (or more precisely in which they could be thermodynamically more stable than the well-known tilted phases of BFO) are not clear. In addition, the possible role played by the oxygen octahedra tilts—that are rather strong in BFO, as evidenced by a tilt angle of 13° in the bulk—has been mostly underestimated. It is worth mentioning that usually, hydrostatic pressure favors oxygen tilts in perovskites, exactly as seen in BFO bulk, whose high-pressure phase loses its ferroelectricity but still exhibits strong oxygen tilts.¹⁷ Moreover, recent calculations also underlined the key role played by the oxygen octahedra tiltings in this system, stressing their interplay with the polar displacements¹⁸ and the magnetic order parameter.¹⁹

In a previous study,¹⁸ we have experimentally shown that BFO epitaxially grown on $[001]$ -oriented LaAlO₃ exhibits a giant tetragonal-like *c/a* ratio around 1.23, with a nonzero in-plane and out-of-plane component of the polarization, which definitely excludes the tetragonal phase and, at that time, we rather suggested a monoclinic phase with either the nontilted *Cm* or the tilted *Cc* space group.

In this work, we present the results of extended *ab initio* density-functional calculations, simulating various BFO phases under compressive misfit strains, by considering the two structural degrees of freedom allowed by the perovskite structure, namely, the polar displacements and the oxygen octahedra tilts. We show that indeed the most stable phases are of monoclinic symmetry and, more interestingly, that the

two phases Cm and Cc are both (meta)stable under such mechanical boundary conditions, with the nontilted one (Cm) being favored at very large compressive strain while the tilted one (Cc) is favored at smaller misfit strains. We also performed synchrotron x-ray diffraction experiments on BFO thin films grown on [001]-oriented LaAlO₃ (LAO) and SrTiO₃ (STO) substrates, which are consistent with our theoretical findings. Our work also further demonstrates the role played by the oxygen tilts which are found to compete, and more precisely, to fight against the polarization. This finding is in agreement with the rather weak enhancement of the polarization observed and reported in the literature and should be taken into account in most multiferroic compounds since they usually present oxygen tilts.

II. COMPUTATIONAL AND THEORETICAL DETAILS

Our density-functional calculations²⁰ have been performed using the *ab initio* total-energy and molecular-dynamics program VASP (Vienna *ab initio* simulation program) developed at the Institut für Materialphysik of the Universität Wien,^{21–24} and the SIESTA (Refs. 25 and 26) program, both leading to similar and very consistent results. They include semicore electrons ($5d^{10}$ for Bi and $3p^6$ for Fe) in the valence. We have used the local-density approximation (LDA), with and without the so-called $+U$ (Hubbard-type) correction [$U=3.87$ eV (Ref. 8)] and the generalized gradient approximation in the form proposed by Perdew, Burke, and Ernzerhof²⁷ (GGA-PBE). We use a 20-atom supercell in which a G-type antiferromagnetic state is constrained, under the assumption of colinear magnetism. Preliminary tests performed on bulk $R3c$ BiFeO₃ provided results in excellent agreement with the literature for both approximations (lattice constant, atomic positions, magnetic moment, etc.).

We simulate bismuth ferrite under [001] epitaxial strain according to the scheme defined, for instance, in Ref. 28: the epitaxial strain enforced by a cubic substrate with [001] orientation leads to $\eta_1 = \eta_2 = \eta$ (in-plane components of the strain tensor), whose value is imposed by the substrate, and $\eta_6 = 0$. The atomic positions and the other components of the strain tensor η_3 , η_4 , and η_5 are allowed to relax until the atomic forces and the σ_3 , σ_4 , and σ_5 components of the stress tensor are zero (within appropriate numerical criteria). The appropriate thermodynamic potential to describe such systems at $T=0$ K is a mixed strain-stress enthalpy²⁹ that simply reduces to the energy when the above conditions are obtained. Thus we just have to compare the total energies of the optimized configurations to decide whether a phase is more stable than another. Note that LDA+ U does not provide significant modifications of our results with respect to LDA.

Periodic boundary conditions are applied along the three directions. Our theoretical approach to epitaxial strain neither incorporate any surface or interfacial contribution nor any effect related to depolarizing fields.^{30,31} In many cases however, this approach is sufficient to predict accurately the main physical trends of ferroelectric thin films, that appear as strongly related to the epitaxial strain.³² Note that we calculate the misfit strain, ξ , for a given in-plane lattice constant a ,

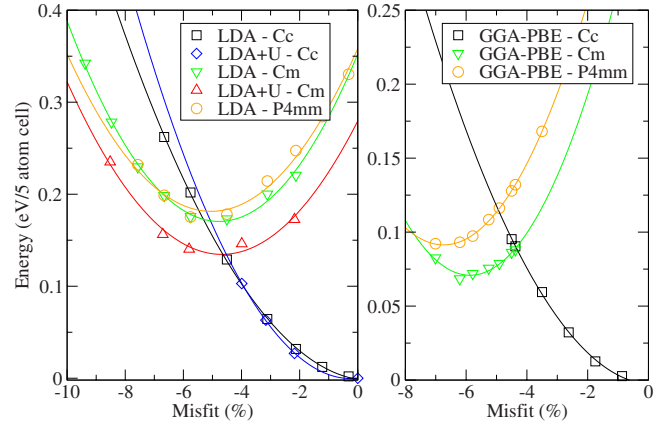


FIG. 1. (Color online) Energy versus misfit strain for the different phases studied in this work, in the LDA (left panel) and GGA-PBE (right panel). The lines are guide for the eyes.

with respect to the theoretical lattice constant a^{th} of $R3c$ BFO (-1.4% in LDA, $+1.8\%$ in GGA-PBE with respect to the experimental lattice constant, as expected), as $\xi = (a - a^{\text{th}}) / a^{\text{th}}$. In other words, our zero misfit strain does *not* correspond to the experimental lattice constant of BFO. Finally, we have evaluated the polarization from the computed relaxed atomic displacements and from the Born effective charges given in Ref. 33 (the values have been confirmed through Berry-phase calculations on selected configurations).

III. COMPUTATIONAL RESULTS

We have first tested several possible solutions having polar displacements and/or oxygen octahedra tilts. However, the lowest energies were obtained for monoclinic symmetries. In Fig. 1, we plot the total energy of Cc , Cm , and $P4mm$ phases as a function of the misfit ξ . The state obtained for a zero misfit (very close to the $R3c$ phase) serves as reference (zero of the energies) for each exchange-correlation functional used (LDA, LDA+ U , and GGA). As one may expect by growing a bulklike $R3c$ phase onto a [001]-oriented substrate, Cc has its minimum for $\xi=0$. Its energy increases with $|\xi|$ and crosses that of Cm for a critical misfit ξ_c that depends on the approximation used ($\approx -5.5\%$ in LDA versus -4.5% in GGA-PBE). Cm and $P4mm$ have their minimum (ξ_{Cm} and ξ_{P4mm}) for $\xi < 0$, as already reported in the literature,¹⁵ and Cm is more stable than $P4mm$ in all cases. Nevertheless for very large (negative) misfits, the in-plane component of the polarization in Cm is suppressed so that $P4mm$ and Cm become identical, i.e., $P4mm$ can be favored. Thus for $\xi < \xi_c$, the monoclinic nontilted phase Cm is more stable than Cc whereas for $\xi > \xi_c$, the monoclinic tilted phase Cc is the lowest-energy phase. These results suggest that, provided that a coherent epitaxy can be realized for very large compressive misfits $\xi < \xi_c$, a nontilted phase of BFO with Cm symmetry is likely to appear in BFO thin films. For these negative misfits, the Cc phase is of course under compressive stress but we point out that paradoxically, for $\xi_{Cm} < \xi < \xi_c$, the BFO films, with Cm phase, exhibit a tensile (rather than compressive) stress.

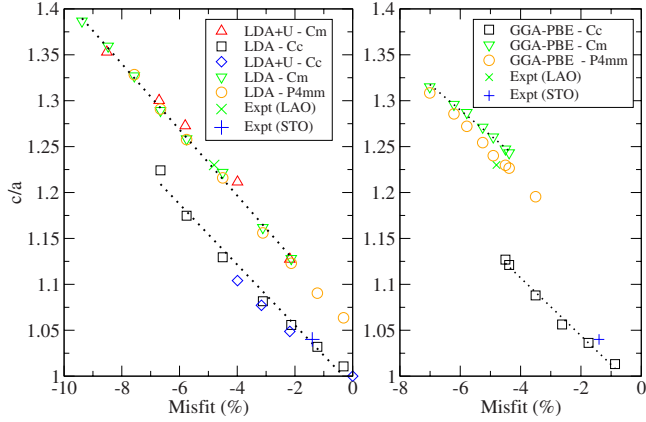


FIG. 2. (Color online) c/a ratio as a function of the misfit strain for the Cc , Cm , and $P4mm$ phases, as obtained from the LDA and LDA+ U (left panel) and from the GGA (right panel). The lines are guide for the eyes.

The nontilted Cm phase is rather similar to the tetragonal $P4mm$ phase, in the sense that it exhibits giant polar out-of-plane displacements that lead to a very large out-of-plane component of the polarization. For example, at $\approx -4.4\%$ (roughly the misfit on LAO, see hereafter), the alternating Fe-O distances along z are 2.92 and 1.88 Å (GGA values) while the in-plane Fe-O distances are 2.00 and 2.04 Å (this slight difference reflects the small in-plane component of \vec{P}). This makes the Fe atoms to be located inside very distorted oxygen octahedra, with one of the oxygen atom among the six forming the octahedron not in the first-neighbor Fe coordination sphere any more. We note that for this misfit, the LDA, unlike the GGA, predicts the Cc phase as the most stable while below $\approx -5.5\%$, Cm becomes more stable but quasi-identical to $P4mm$ in this approximation. The monoclinic angle is smaller than 1° for Cc (LDA and GGA). For Cm , it is about $1^\circ - 2^\circ$ (LDA) and a bit more in the GGA ($2^\circ - 3^\circ$).

The c/a ratio increases with $|\xi|$ as expected with compressive in-plane strains (Fig. 2). Its evolution is roughly linear for both phases, with c/a for Cm and $P4mm$ much larger than that of Cc by about 0.06. The most striking feature is that the amplitude of the polarization in the Cc phase remains approximately constant ($\approx 80 - 90 \mu\text{C}/\text{cm}^2$) between $\xi = 0\%$ and -4% (Fig. 3) which is in good agreement with Ref. 16. As indicated by Fig. 3, between these two strain values, \vec{P} simply rotates, with its out-of-plane component P_\perp becoming progressively higher than its in-plane component P_\parallel . Above $\xi = -4\%$, the total amplitude of \vec{P} starts to increase slowly to reach a value of $\approx 95 \mu\text{C}/\text{cm}^2$ for $\xi = -6\%$. In contrast, the variation in the polarization in Cm is much more sensitive to the misfit strain since already at $\xi = -2\%$, the polarization has a value of $\approx 115 \mu\text{C}/\text{cm}^2$. This result reveals the strong impact of the presence of the oxygen tilts which fight against the natural enhancement of the out-of-plane polarization because of the compressive in-plane strain. The P_\perp component of Cm is much higher than its P_\parallel and increases with $|\xi|$ (from $\approx 100 \mu\text{C}/\text{cm}^2$ up to $\approx 140 \mu\text{C}/\text{cm}^2$ for $\xi = -6\%$) while the in-plane component of Cm progressively decreases to zero giving rise to a tetragonal-like total polarization.

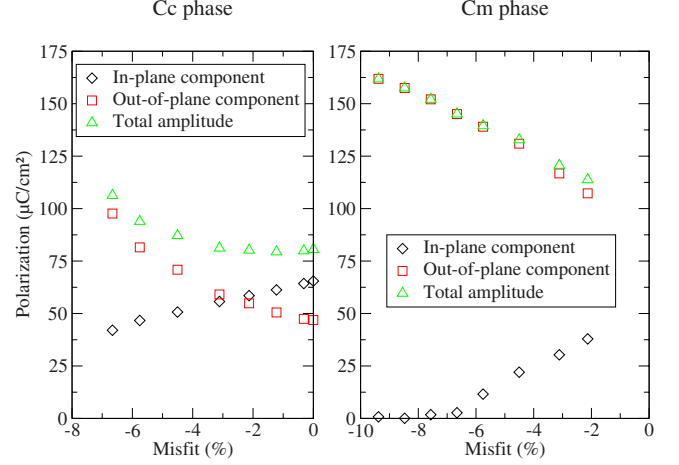


FIG. 3. (Color online) In-plane component, out-of-plane component, and total amplitude of the polarization as a function of misfit for Cc and Cm phases. LDA results (the GGA curves look very similar).

IV. EXPERIMENTAL RESULTS

Our theoretical investigation thus reveals that two monoclinic phases might exist in BFO films depending on the value of the misfit strain: Cm at strong misfit and Cc at small misfit. To confirm such unexpected results, we decided to undertake an experimental work with two substrates that could correspond to these different conditions, namely, LAO(001) ($\xi_{\text{LAO}} = -4.8\%$) and STO(001) ($\xi_{\text{STO}} = -1.4\%$). The samples have been epitaxially grown by pulsed laser deposition on these two substrates and exhibit a monoclinic symmetry as already reported.¹⁸ The c/a ratio measured, i.e., 1.23 and 1.04 for the LAO and STO substrates, respectively, are reported in Fig. 2: a perfect agreement with the theoretical results is obtained with the Cc and Cm states for STO and LAO substrates, respectively, which therefore suggests the existence of a *different* monoclinic phase for each sample. Note that on the LAO substrate, we found that different phases states can be obtained depending on the growth process, as the related misfit strain is at the boundary between the Cc and Cm phases. As a result, different values of the polarization can be experimentally obtained using such a substrate.¹⁸

The Cm and the Cc phases distinguish themselves by the absence versus presence of oxygen octahedra tilts, respectively. Interestingly, these oxygen octahedra can be revealed by the presence of superstructure peaks using diffraction techniques. Whereas neutron diffraction appears to be the most appropriate tool because of its sensitivity to light oxygen atoms, it has the default to be also sensitive to the magnetic order, which in BFO gives rise to superstructure peaks at the same positions to those associated with the tilts. Therefore, we rather performed an x-ray diffraction study using a synchrotron radiation, which is insensitive to the magnetic order and powerful enough to detect oxygen tilt superstructure peaks, if they exist. The x-ray diffraction experiment was carried out on the six-circle diffractometer of the CRISTAL beamline at SOLEIL (France) at room temperature, using a 8 keV ($\lambda = 1.54059 \text{ \AA}$) radiation. While several super-

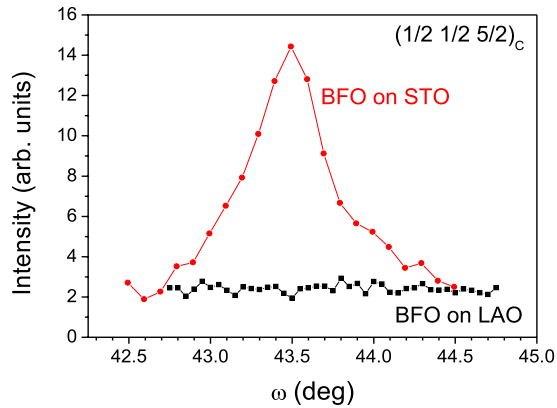


FIG. 4. (Color online) XRD pattern of $1/2$, $1/2$, and $5/2$ superstructure peaks on STO and LAO. The intensity of the LAO $1/2$, $1/2$, and $5/2$ confirms that epitaxially grown BFO on LAO has no antiferrodistortion along $1/2$, $1/2$, and $1/2$ direction.

structure peaks compatible with a Cc phase have been evidenced for BFO onto STO, none was detected for BFO onto LAO. As an illustration, we plotted on Fig. 4 the $(\frac{1}{2}, \frac{1}{2}, \frac{5}{2})$ superstructure peak detected for BFO onto STO and the intensity measured, in the same experimental conditions (time of exposure, beam size, etc., ...) for BFO onto LAO, for which no peak can be obviously observed. From the comparison, we draw the conclusion that the octahedral tilts in BFO on LAO are absent or too weak to be detected. These experimental results therefore strongly support our theoretical predictions that, for the misfit $\xi_{\text{LAO}} = -4.8\%$, the phase has the nontilted Cm space group while the tilted Cc phase describes the structure associated with $\xi_{\text{STO}} = -1.4\%$.

V. CONCLUSION

In summary, combining experimental and theoretical approaches, we found, for relatively low compressive strain (e.g., BFO grown onto STO), that BFO adopts a tilted Cc monoclinic phase whereas a nontilted Cm monoclinic phase is favored for larger compressive strain (e.g., BFO grown onto LAO). Beyond the competition between these two monoclinic phases, the energy curves of Fig. 1 suggest the possibility of coexisting phases. In such conditions with coexisting competing states, an external electric field might induce giant effects. The main difference between these monoclinic phases is the presence of octahedral tilts in Cc . The polarization associated with this Cc phase is strongly coupled to the oxygen tilts and cannot evolve freely. It is not enhanced by the compressive misfit between 0% and -4%. The interplay between polar displacements and oxygen tilts (which are the two structural degrees of freedom that usually exclude each other in perovskites) is of strong interest in many multiferroics since both degrees of freedom can coexist in these latter fascinating systems.

ACKNOWLEDGMENTS

L.B. acknowledges the ONR under Grants No. N00014-04-1-0413 and No. N00014-08-1-0915, NSF under Grants No. DMR 0701558 and No. DMR-0404335, and DOE under Grant No. DE-SC0002220. S.L. acknowledges the support from the University of South Florida under Grant No. R074021. Partial financial support by EU STREP Macomufi, ANR Pnano (Méloïc project), C-Nano Ile de France (Magellan project), and PRES Universud is acknowledged. We acknowledge SOLEIL for provision of synchrotron radiation facilities and we would like to thank Erik Elkaim and Fabien Legrand for assistance in using beamline CRISTAL.

¹M. Fiebig, *J. Phys. D* **38**, R123 (2005).

²K. F. Wang, J.-M. Liu, and Z. F. Ren, *Adv. Phys.* **58**, 321 (2009), and references therein.

³J. F. Scott, *Nature Mater.* **6**, 256 (2007).

⁴M. Gajek, M. Bibes, S. Fusil, K. Bouzehouane, J. Fontcuberta, A. Barthélémy, and A. Fert, *Nature Mater.* **6**, 296 (2007).

⁵M. Bibes and A. Barthélémy, *Nature Mater.* **7**, 425 (2008).

⁶W. Eerenstein, N. D. Mathur, and J. F. Scott, *Nature (London)* **442**, 759 (2006).

⁷R. Ramesh and N. A. Spaldin, *Nature Mater.* **6**, 21 (2007).

⁸I. A. Kornev, S. Lisenkov, R. Haumont, B. Dkhil, and L. Bellaiche, *Phys. Rev. Lett.* **99**, 227602 (2007).

⁹G. Catalan and J. F. Scott, *Adv. Mater.* **21**, 2463 (2009), and references therein.

¹⁰D. Lebeugle, D. Colson, A. Forget, and M. Viret, *Appl. Phys. Lett.* **91**, 022907 (2007).

¹¹P. Fischer, M. Polomska, I. Sosnowska, and M. Szymanski, *J. Phys. C* **13**, 1931 (1980).

¹²H. Bea, M. Bibes, S. Petit, K. Kreisel, and A. Barthélémy, *Philos. Mag. Lett.* **87**, 165 (2007).

¹³A. J. Hatt, N. A. Spaldin, and C. Ederer, *Phys. Rev. B* **81**,

054109 (2010).

¹⁴C. Ederer and N. A. Spaldin, *Phys. Rev. Lett.* **95**, 257601 (2005).

¹⁵D. Ricinschi, K.-Y. Yun, and M. Okuyama, *J. Phys.: Condens. Matter* **18**, L97 (2006).

¹⁶H. W. Jang, S. H. Baek, D. Ortiz, C. M. Folkman, R. R. Das, Y. H. Chu, P. Shafer, J. X. Zhang, S. Choudhury, V. Vaithyanathan, Y. B. Chen, D. A. Felker, M. D. Biegalski, M. S. Rzchowski, X. Q. Pan, D. G. Schlom, L. Q. Chen, R. Ramesh, and C. B. Eom, *Phys. Rev. Lett.* **101**, 107602 (2008).

¹⁷R. Haumont, P. Bouvier, A. Pashkin, K. Rabia, S. Frank, B. Dkhil, W. A. Crichton, C. A. Kuntscher, and J. Kreisel, *Phys. Rev. B* **79**, 184110 (2009).

¹⁸H. Béa, B. Dupé, S. Fusil, R. Mattana, E. Jacquet, B. Warot-Fonrose, F. Wilhelm, A. Rogalev, S. Petit, V. Cros, A. Anane, F. Petroff, K. Bouzehouane, G. Geneste, B. Dkhil, S. Lisenkov, I. Ponomareva, L. Bellaiche, M. Bibes, and A. Barthélémy, *Phys. Rev. Lett.* **102**, 217603 (2009).

¹⁹S. Lisenkov, D. Rahmedov, and L. Bellaiche, *Phys. Rev. Lett.* **103**, 047204 (2009).

²⁰W. Kohn and L. J. Sham, *Phys. Rev.* **140**, A1133 (1965).

- ²¹G. Kresse and J. Hafner, *Phys. Rev. B* **47**, 558 (1993); **49**, 14251 (1994).
- ²²G. Kresse and J. Furthmüller, *Comput. Mater. Sci.* **6**, 15 (1996).
- ²³G. Kresse and J. Furthmüller, *Phys. Rev. B* **54**, 11169 (1996).
- ²⁴G. Kresse and D. Joubert, *Phys. Rev. B* **59**, 1758 (1999).
- ²⁵P. Ordejon, E. Artacho, and J. M. Soler, *Phys. Rev. B* **53**, R10441 (1996).
- ²⁶J. M. Soler, E. Artacho, J. D. Gale, A. García, J. Junquera, P. Ordejon, and D. Sánchez-Portal, *J. Phys.: Condens. Matter* **14**, 2745 (2002).
- ²⁷J. P. Perdew, K. Burke, and M. Ernzerhof, *Phys. Rev. Lett.* **77**, 3865 (1996).
- ²⁸O. Diéguez, K. M. Rabe, and D. Vanderbilt, *Phys. Rev. B* **72**, 144101 (2005).
- ²⁹N. A. Pertsev, A. G. Zembilgotov, and A. K. Tagantsev, *Phys. Rev. Lett.* **80**, 1988 (1998).
- ³⁰B.-K. Lai, I. Kornev, L. Bellaiche, and G. Salamo, *Appl. Phys. Lett.* **86**, 132904 (2005).
- ³¹O. Diéguez, S. Tinte, A. Antons, C. Bungaro, J. B. Neaton, K. M. Rabe, and D. Vanderbilt, *Phys. Rev. B* **69**, 212101 (2004).
- ³²K. M. Rabe, *Curr. Opin. Solid State Mater. Sci.* **9**, 122 (2005).
- ³³J. B. Neaton, C. Ederer, U. V. Waghmare, N. A. Spaldin, and K. M. Rabe, *Phys. Rev. B* **71**, 014113 (2005).